UC Berkeley
UC Berkeley Previously Published Works

Title

Aseismic Transform Fault Slip at the Mendocino Triple Junction From Characteristically Repeating Earthquakes

Permalink

https://escholarship.org/uc/item/9sv2h50v

Journal

Geophysical Research Letters, 45(2)

ISSN

0094-8276

Authors

Materna, Kathryn
Taira, Taka'aki
Bürgmann, Roland

Publication Date

2018-01-28

DOI

10.1002/2017gl075899

Peer reviewed

Aseismic Transform Fault Slip at the Mendocino Triple Junction From Characteristically Repeating Earthquakes

[Kathryn Materna](#)

[Taka'aki Taira](#)

[Roland Bürgmann](#)

SECTIONS

PDF

TOOLS

SHARE

Abstract

The Mendocino Triple Junction (MTJ), at the northern terminus of the San Andreas Fault system, is an actively deforming plate boundary region with poorly constrained estimates of seismic coupling on most offshore fault surfaces. Characteristically repeating earthquakes provide spatial and temporal descriptions of aseismic creep at the MTJ, including on the oceanic transform Mendocino Fault Zone (MFZ) as it subducts beneath North America. Using a dataset of earthquakes from 2008 to 2017, we find that the easternmost segment of the MFZ displays creep during this period at about 65% of the long-term slip rate. We also find creep at slower rates on the shallower strike-slip interface between the Pacific plate and the North American accretionary wedge, as well as on a fault that accommodates Gorda subplate internal deformation. After a nearby M5.7 earthquake in 2015, we observe a possible decrease in aseismic slip on the near-shore MFZ that lasts from 2015 to at least early 2017.

1 Introduction

Seismic coupling on many faults is known to be spatially and temporally variable, but what controls seismic coupling remains an open question in tectonics (Avouac, [2015](#)). As a result of variations in seismic coupling, fault segments may creep aseismically as a mechanism of moment release at any stage of the earthquake cycle. Factors proposed to influence the creeping behavior of faults include the frictional properties of fault zone rocks, loading rate, temperature, fault surface geometry, and pore fluid pressure (Avouac, [2015](#); Harris, [2017](#); Scholz, [1998](#)).

Determining spatiotemporal variations in creep rates on a variety of faults and in many tectonic settings is key to approaching the general question of factors promoting creeping fault behavior.

Oceanic transform faults are one class of faults that may give insight into fault creep processes (Abercrombie & Ekström, 2001). In contrast to continental faults, oceanic transform faults juxtapose relatively homogenous lithosphere, making them simpler geologic systems in which to study creeping faults. Research suggests that oceanic transform faults are especially likely to display creep due to the presence of fluids in the crust and the hydration of ultramafic minerals in the mantle (Boettcher & Jordan, 2004; Frohlich & Wetzel, 2007; McGuire et al., 2005). Hydrated minerals such as serpentine and talc contribute to velocity-strengthening frictional behavior, and the presence of fluids may promote creep by reducing the effective normal stress on faults and enhancing pressure solution creep (Harris, 2017). Boettcher and Jordan (2004) evaluate a global dataset of historical seismic moment release along 65 oceanic transform faults and determine an average seismic coupling coefficient (ratio of seismic to total slip above the 600°C isotherm) of 0.15 ± 0.05. Evidence of earthquake swarms, foreshock sequences, and dynamically triggered seismicity on oceanic transforms also suggests that creep on these systems may be highly time-dependent (Cattania et al., 2017; McGuire et al., 2005).

In northern California, the Mendocino Fault Zone (MFZ) provides an opportunity to study fault creep on an oceanic transform fault located close to land. This transform fault is part of the Mendocino Triple Junction (MTJ), the region where the North American plate, Pacific plate, and Gorda subplate meet (Figure 1a). In this area, the Gorda subplate, the southern portion of the Juan de Fuca plate, subducts obliquely beneath the North American plate at a rate of about 27 mm/yr (DeMets et al., 2010). South of the MTJ, the Pacific plate moves northwest at about 51 mm/yr with respect to North America along the San Andreas fault system (DeMets et al., 2010). The Pacific plate south of the MFZ is overlain by the Vizcaino block, an overthickened piece of crust with origins in the North American accretionary complex (Henstock & Levander, 2003; Leitner et al., 1998). Along the MFZ, the relative motion between the Pacific plate and Gorda subplate, determined from 0.78 Ma magnetic lineations, is about 47 mm/yr oriented west-northwest (DeMets et al., 2010). The relative motion between the three plates results in northward migration of the MTJ (Furlong & Schwartz, 2004) and internal deformation within the Gorda lithosphere (Chaytor et al., 2004; Gulick et al., 2002). In 1992, this area hosted a *M*7.1 mainshock with slip oriented parallel to the plate interface followed by two *M*6.5 aftershocks within the Gorda subplate (Oppenheimer et al., 1993).

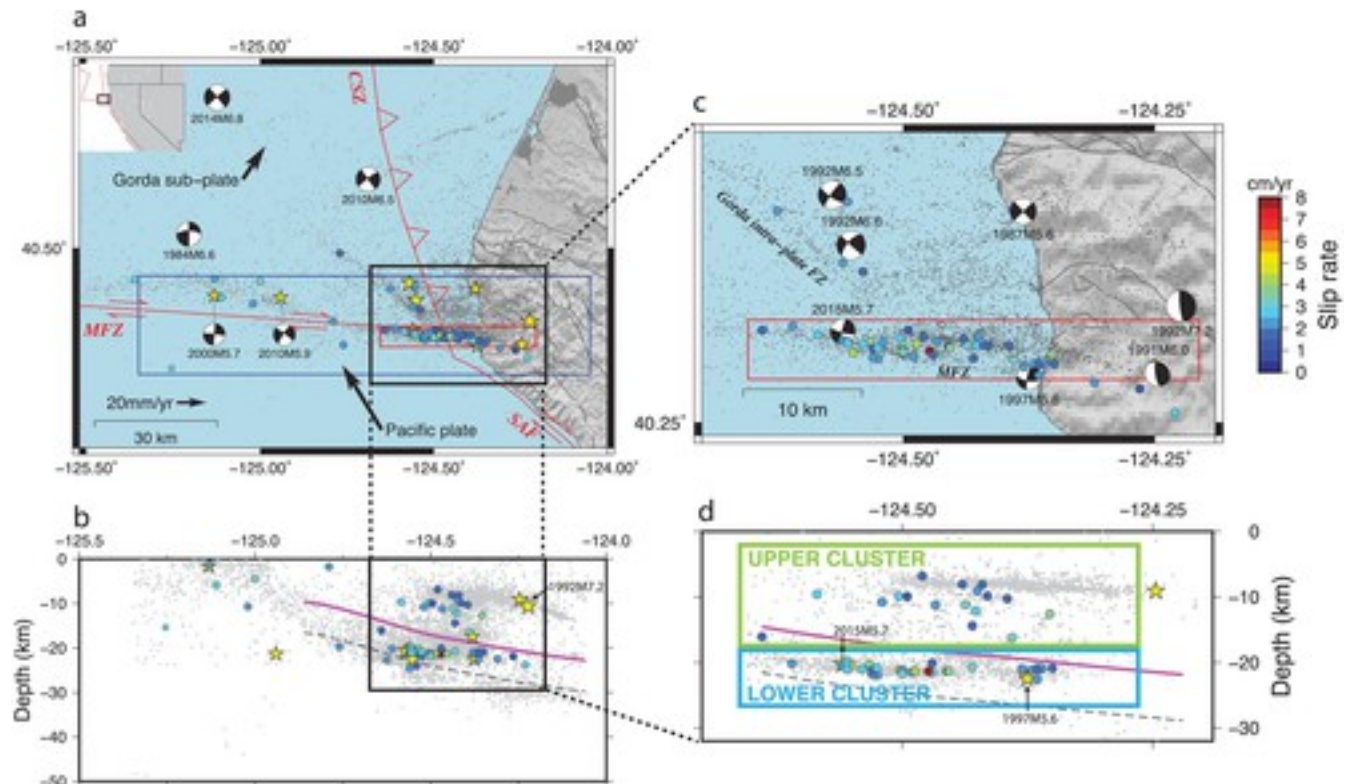**Figure 1**

(a) CREs at the MTJ, where the Mendocino Fault Zone (MFZ), Cascadia Subduction Zone (CSZ), and San Andreas Fault (SAF) intersect. The 1984–2017 background seismicity from a double-difference relocated catalog (Waldhauser & Schaff, 2008) is shown in gray. Especially large previous seismic events are marked by their moment tensors in map view (Table S1; Ekström et al., 2012), and by yellow stars on the cross sections. (b) Depth profile through the blue box in Figure 1a. Each sequence is color coded by inferred slip rate. CRE sequences with double-differenced locations are marked by circles; one sequence with only NCSN locations is shown as a square. The subduction interface model from Slab1.0 (Hayes et al., 2012; McCrory et al., 2012) is shown in magenta, with a dotted line to represent the approximate position of the Moho 7 km deeper than the interface. (c and d) Corresponding close-ups of the central region.

Much of the current research on fault creep relies on geodetic measurements from terrestrial and space geodetic techniques. Seafloor geodetic measurements have been used to study oceanic transform faults (e.g., McGuire & Collins, 2013), but these techniques are still prohibitively challenging. At the MTJ, we instead use characteristically repeating earthquakes (CREs) to identify fault segments with aseismic creep. These microearthquakes with nearly identical waveforms represent repeated ruptures of the same seismic asperity surrounded by an otherwise creeping fault zone (Nadeau & McEvilly, 1997). The local creep rate of a fault segment can be inferred from the timing and magnitude of CREs (Nadeau & Johnson, 1998). CREs have been used to detect fault creep and estimate aseismic slip rates in a variety of tectonic settings (Chen et al., 2007; Dominguez et al., 2016; Meng et al., 2015; Nadeau & McEvilly, 2004; Uchida &

Matsuzawa, [2011], [2013]; Yao et al., [2017]). Several examples of CREs with overlapping rupture areas have been detected along the MFZ (Waldhauser & Schaff, [2008]). Here we use this approach to identify creeping fault structures in the MTJ and explore the recent spatiotemporal distribution of aseismic slip on the MFZ.

2 Methods

In order to detect CREs, we use seismic waveform data from eight Plate Boundary Observatory (PBO) borehole stations (~150–200 m depth) and five surface broadband stations in the Cape Mendocino area (Figure S1 in the supporting information). All waveforms have a sampling frequency of 100 Hz. The PBO borehole geophones were installed in late 2008 and provide the bulk of the data for this study. We investigate over 120,000 waveform records from 18,000 earthquakes between October 2008 and July 2017 in the Northern California Seismic Network (NCSN) catalog. Waveforms in the vertical component were extracted from the Northern California Earthquake Data Center (NCEDC) continuous data. The instrument responses were corrected to obtain velocity waveforms, and a high-pass filter of 0.5 Hz was applied to suppress microseismic noise. We select waveforms for each event from 30 s before the *P* wave arrival to 20 s after the *P* wave arrival.

We identify repeating earthquake pairs within this dataset based on waveform similarity. We compute the mean frequency-domain coherence for each event pair with locations less than 30 km apart across a frequency band between 0.5 Hz and a maximum of 15 Hz. For events with low signal-to-noise ratio (SNR), we reduce the relevant frequency band to only include the frequencies at which both events have SNR greater than 5.0. If the mean coherence across this frequency band is greater than 0.97 at two or more stations, then we determine that the event pair is a repeating pair. We then group repeating earthquake pairs into sequences that share common events (Uchida & Matsuzawa, [2013]). The method employed in this study is similar to a CRE detection algorithm used for small repeating subduction events offshore Japan (Uchida et al., [2009]; Uchida & Matsuzawa, [2013]), but with the additional requirement that the SNR > 5 for each event pair. As most CREs at the MTJ are offshore and small magnitude, this modified approach improves reliability by rejecting the attenuated or noisy parts of the seismic signal when making CRE detections (supporting information Text S1; Chen et al., [2013]; Tormann et al., [2014]).

We estimate the slip rate of all CRE sequences that span more than 1 year in total duration. By removing short-lived sequences, we avoid biasing the slip rate estimates with burst-type repeaters that do not reflect the tectonic loading rate (e.g., Templeton et al., [2008]). We use the

empirical scaling relationship of Nadeau and Johnson ([1998](#)), derived from small repeating earthquakes in Parkfield, California, to relate the occurrence of CREs to cumulative slip history:

$$\log(d) = -2.36 + 0.17 \log(M_0), \quad (1)$$

where the slip d is in centimeters and the moment M_0 is in dyne-centimeters.

Although this scaling equation is empirically calibrated for Parkfield, comparisons of geodetic and CRE-derived creep rates elsewhere suggest that this relationship holds well in different tectonic regimes around the world, such as California, Taiwan, Japan, and Tonga-Vanuatu, among others (e.g., Chen et al., [2007](#); Uchida & Matsuzawa, [2013](#); Yu, [2013](#)). Based on these existing comparisons, we make the assumption that this empirically calibrated scaling relationship sufficiently describes slip history inferred at the MTJ from repeating earthquakes. Even if this assumption is not valid, trends in CRE activity should reveal any time-dependent slip behavior at the MTJ. The [supporting information](#) (Figures [S3–S7](#)) contains analysis of the sensitivity of our results to the coherence cutoff and frequency band used in CRE detection.

3 Results

3.1 Spatial Distribution of Repeating Earthquakes

Applying this method to northern California events west of 123.3°W, we find 83 CRE sequences, with average magnitudes between 1.5 and 3.0. Many sequences are located on a narrow and well-defined surface that trends east-west at 40.3°N (Figure [1](#)a), closely aligned with the MFZ and its eastward continuation below land. In particular, the CRE sequences on this surface are separated into an upper cluster at 10–17 km depth, and a lower cluster at 18–25 km depth (Figure [1](#)d). We separate these two distinct clusters of seismicity in our subsequent analysis.

The lower cluster lies below the CSZ plate interface of McCrory et al. ([2012](#)), suggesting that it is located between the oceanic Pacific plate and the Gorda subplate. Composite focal mechanisms computed for CRE sequences in the lower cluster show overall right-lateral strike-slip movement (Figure [S8](#)), consistent with the moment tensors of nearby M5.6 and M5.7 earthquakes in 1997 and 2015 (Figure [1](#)c).

The upper cluster (between 10 km and 17 km depth) lies above the inferred CSZ plate interface, placing it along the North American accretionary wedge. Composite focal mechanisms for the upper cluster also show dominantly right-lateral strike slip on east-west striking nodal planes (Figure [S8](#)).

Outside of the narrow structure that contains most of the CREs, we detect several sequences on a northwest-southeast striking intraplate fault in the Gorda subplate (Figure 1c). These sequences are located at depths of 15–25 km. Their focal mechanisms are poorly constrained, but historical focal mechanisms for M3-M4 events on that structure show dextral strike slip. We also detect several CRE sequences further west on the MFZ, which tend to contain larger-magnitude ($M \sim 3$) events with poorly constrained depths (Figure 1a). We do not detect CREs east of 124°W or on the subduction thrust.

3.2 Creep Rates and Time-Dependent Creep

We compute average slip rates for the upper and lower clusters on the MFZ by summing the slip inferred from each CRE and dividing by the total number of CRE sequences in each region (Nadeau & McEvilly, 2004). This technique helps to reduce some of the uncertainty in individual sequence slip rates under the assumption that the CREs are driven by spatially coherent aseismic slip. In the upper cluster (Figure 1d), we find 17 CRE sequences and infer an average slip rate of about 23 ± 4 mm/yr. The lower cluster contains a more active and variable set of 38 CRE sequences with an average slip rate of 29 ± 12 mm/yr over the observed time window. The average slip rate of CRE sequences west of ~124.6°W on the MFZ is about 27 ± 3 mm/yr.

Several time-variable features of the dataset highlight differences in behavior between the upper and lower clusters. We note that the background seismicity in the two regions responds differently to two regional earthquakes (Figure 2). In the upper cluster, aftershock activity is observed following a 2014 M6.8 strike-slip earthquake 100 km to the northwest, while in the lower cluster, aftershock activity is observed following the nearby 2015 M5.7 event. The most notable potential slip rate variation is observed in the lower cluster surrounding the 2015 M5.7 event (Figure 2d). There appears to be faster slip for about 6 months before this earthquake, and 2 years of relative quiescence afterward. The M5.7 earthquake occurred on the western edge of the lower cluster (Figure 3) and has a similar focal mechanism to many of the composite CREs. We conservatively estimate the rupture patch of this event to be about 9 km in length by 6 km wide (Wells & Coppersmith, 1994). Preliminary modeling of this event using empirical Green's functions suggests a smaller patch with a ~6 km long rupture and 7 MPa stress drop (Jianhua Gong, personal communication, 2017), consistent with other findings that MFZ earthquakes have higher-than-average stress drops (e.g., 5–20 MPa from Chen & McGuire, 2016). The spatial and temporal relationship between this M5.7 earthquake and the CRE sequences is shown in Figure 3.
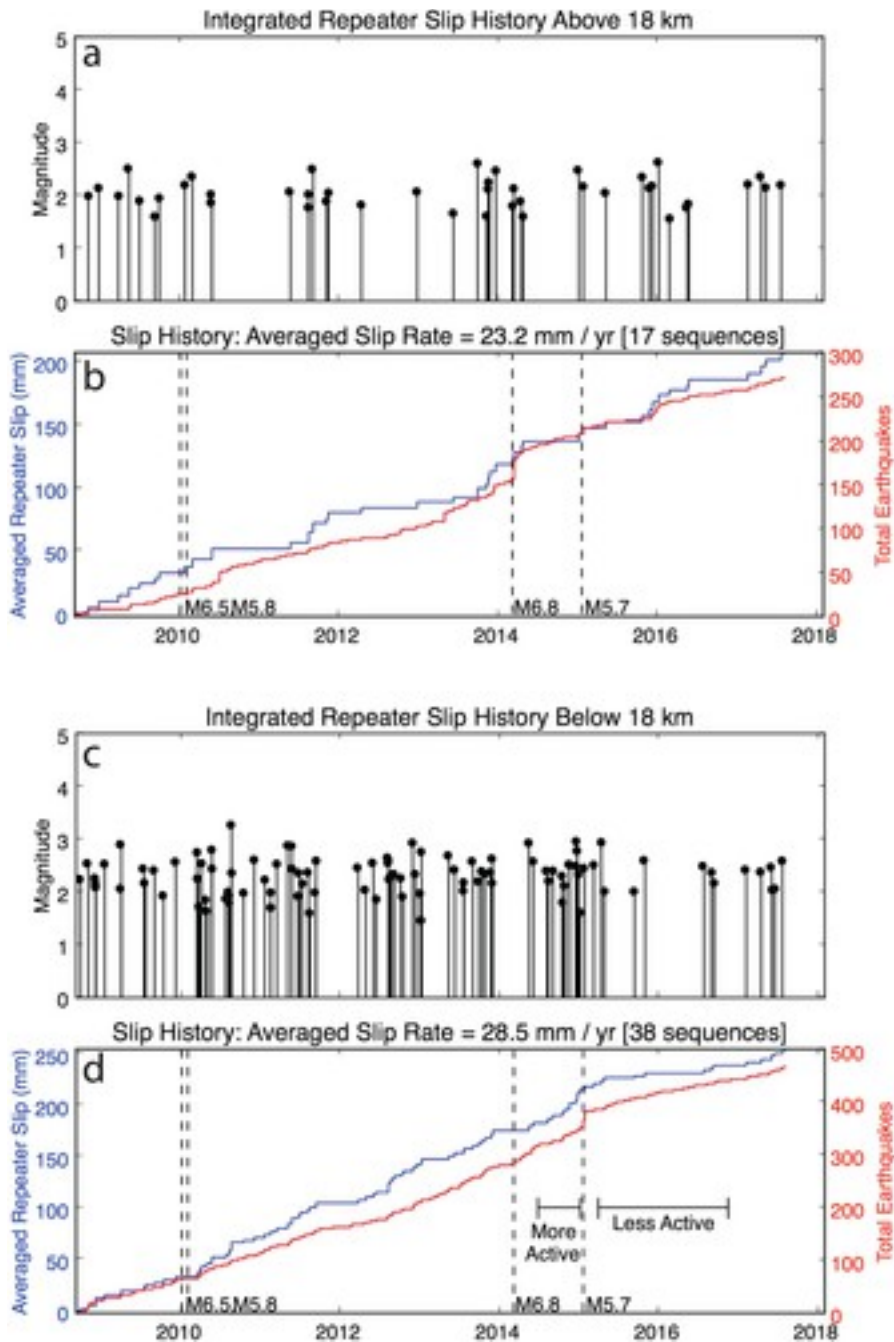
Figure 2

(a and b) History of CRE activity in the upper cluster, 10–17 km depth (Figure 1d). (c and d) History of CRE activity in the lower cluster, 18–25 km depth (Figure 1d). Blue lines represent cumulative slip inferred from CREs with equation 1. Black dashed lines show occurrence times of nearby moderate earthquakes (see Figure 1 for locations); the red curves show the cumulative number of events in the double-differenced catalog within the regions of interest.
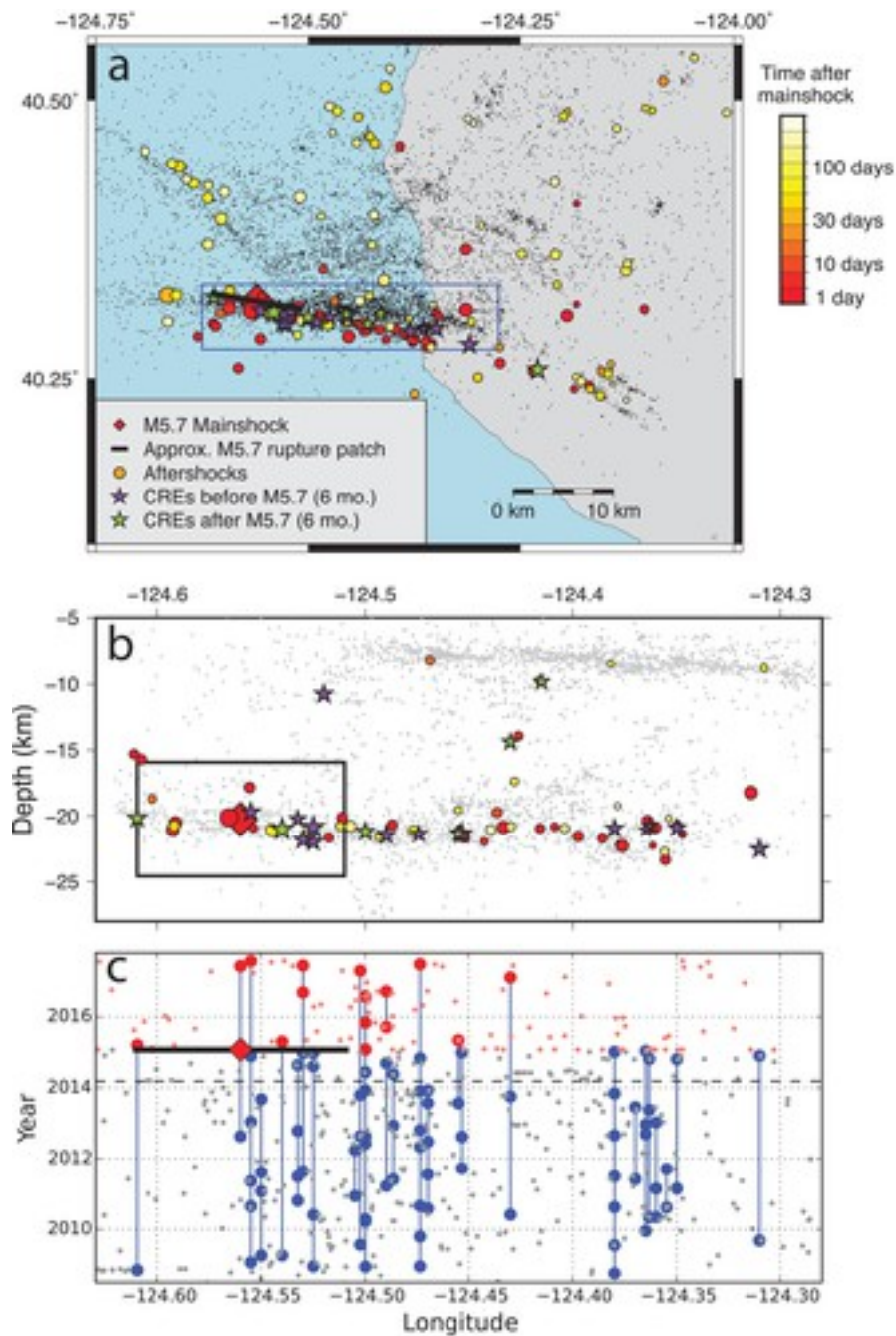
Figure 3

Evolution of the 2015 M5.7 earthquake sequence (double-differenced hypocenter marked by red diamond). The first-order rupture patch dimensions based on Wells and Coppersmith (1994) are shown in black. (a) Map view of the earthquake sequence. Double-differenced background seismicity (1984–2017) is shown in black dots. Aftershocks of the 2015 event are shown as filled circles color coded by time, ranging from the day of the mainshock (red) to up to 6 months later (yellow). Purple and green stars show the locations of CRE activity in the 6 months before and after the earthquake respectively. (b) Cross-sectional view of the blue box in Figure 3a. (c) Time-space plot of the CRE sequences in the blue box in Figure 3a at 18–35 km depth; this depth

range corresponds to the "lower cluster" in Figure 1. Sequences of CREs are shown as large dots connected by vertical lines, while background seismicity is marked by small dots. The red-blue color change indicates when the 2015 M5.7 earthquake occurred. The horizontal dashed line indicates the time of a M6.8 earthquake located 85 km to the northwest (Figure 1).

4 Discussion

Our data show evidence for multiple robust sequences of CREs in the MTJ, which we interpret as representing aseismic slip on several fault structures between 2008 and 2017 (Figure 4a). At 20–30 km deep, the highly active CRE sequences (Figure 1d, lower cluster) reflect aseismic creep between the Pacific plate and the subducting Gorda subplate. In this area, the background microseismicity in the downgoing slab illuminates a previously documented double seismic zone, whose layers are thought to result from dehydration embrittlement of the upper crust and the serpentinized upper mantle, respectively (McCrory et al., 2012; Yamasaki & Seno, 2003). The CREs in this region appear to lie on the southern edge of the Gorda subplate in the depth range between the upper and lower layers of the double seismic zone (Figure 1b), where the downgoing slab abuts the Pacific lithosphere along the eastern extension of the MFZ (McCrory et al., 2012; Wang & Rogers, 1994).
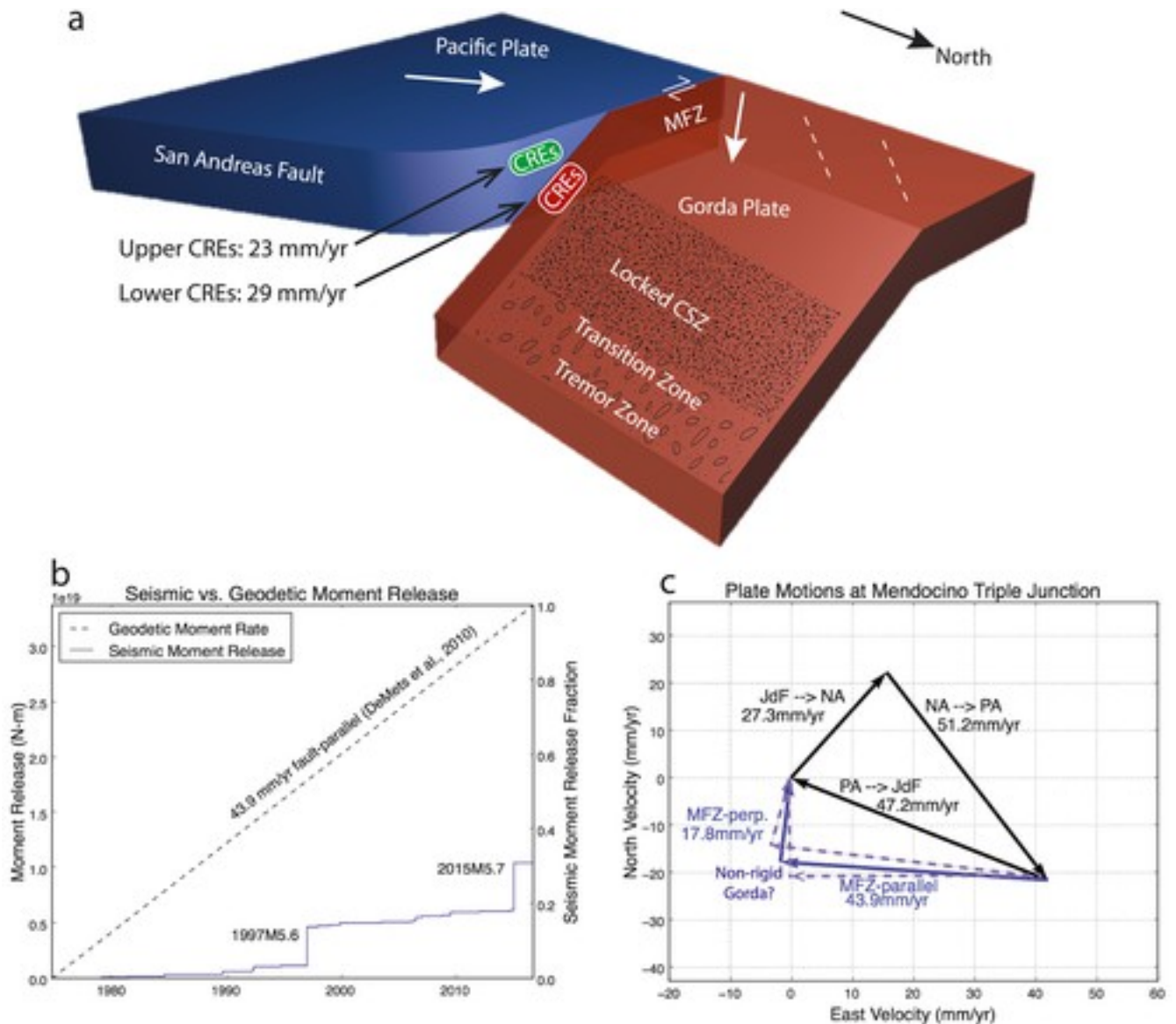
Figure 4

(a) Schematic interpretation of the CRE sequences in the MTJ. This view is from the northeast with the North American plate removed. The red region of CRE activity shows the fastest creep rates (lower cluster in Figure 1d; about 29 mm/yr), while the green region shows creep rates of about 23 mm/yr. (b) Long-term moment accumulation versus seismic moment release on the MFZ (lower cluster in Figure 1d), showing that approximately 30% of the moment budget in the last 40 years has been released seismically in M > 3.0 earthquakes from the NCSN catalog. (c) Relative motion vectors around the MTJ from the MORVEL 2010 model assuming a rigid Juan de Fuca plate. The blue arrows denote the components of the Pacific/Juan de Fuca relative motion that are parallel and perpendicular to the MFZ, contributing to the dextral slip and shortening across the fault, respectively. When adjusted for internal deformation within the Gorda subplate, relative motion vectors are lower than the MORVEL model in the western segment of the MFZ and higher in the eastern segment.

We interpret the upper cluster of Figure 1d (10–17 km depth) to be above the subducting slab interface, and therefore juxtaposing the Pacific plate and overlying Vizcaino block against the accretionary wedge of the North American plate (Figure 4a). However, the CREs in this range have a patchier spatial distribution. Based on the sparser distribution of CREs, we infer that this part of the transform fault zone more likely contains a heterogeneous distribution of locked and aseismically slipping patches.

We do not see any CRE activity on the plate interface of the CSZ, consistent with previous estimates that it is highly coupled in this region (McCaffrey et al., 2000; Schmalzle et al., 2014). We also do not see spatial overlap between the CRE activity and the deep-seated tremor on the CSZ (Boyarko & Brudzinski, 2010; Wech, 2010), suggesting that CREs and tremor reflect separate slip processes on the shallow transform fault and the deep subduction zone respectively.

We detect several sequences of CREs on a northwest-southeast trending strike-slip fault in the interior of the Gorda subplate (Figures 1c and S5–S7). In the last several decades, large earthquakes up to magnitude 7 have been recorded on strike-slip faults within the Gorda subplate (Rollins & Stein, 2010), including a 2010 *M*6.5 slightly north of the MTJ (Figure 1a). Our results suggest that for the intraplate fault of Figure 1c, some of the deformation budget is also aseismic, although it is difficult to quantify how much given current data. We cannot place constraints on other faults that do not host CREs, as they may be fully locked or creeping without producing detectable CREs.

The inferred 2008–2017 average slip rate of the MFZ from repeating earthquakes is about 29 mm/yr with uncertainties of 12 mm/yr. By comparison, the expected long-term slip rate of the MFZ, derived from seafloor spreading data in MORVEL 2010, is 44 mm/yr (DeMets et al., 2010; Figure 4). Assuming this long-term velocity is representative of the loading rate, only about 30% of the total moment deficit between 18 and 28 km depth has been relieved in recorded earthquakes since 1976 (Figure 4b), leaving 70% of the moment deficit on the MFZ to be accounted for in another fashion, that is, future earthquakes or aseismic slip. Although we cannot characterize the aseismic slip processes before the start of our observations, the CRE results since 2008 lead us to conclude that in recent years, aseismic slip has accommodated a majority of the 70% remaining moment deficit on the MFZ. A caveat, however, relates to the internal deformation of the Gorda subplate and the nonuniform spreading rate on the Gorda ridge (Chaytor et al., 2004; Wilson, 1986, 1989). Taking this adjustment into account, the long-term slip rate on the MFZ may vary from the MORVEL 2010 estimate, with lower slip rates in the west and higher slip rates in the east (Pollitz et al., 2010). Consequently, on the near-shore

segment of the MFZ, we would expect a larger overall moment budget on the MFZ and a smaller aseismic contribution to the moment release.

The 2015 *M*5.7 earthquake shows that the MFZ, although partially creeping, also occasionally generates moderate-sized earthquakes. Estimates of the earthquake's rupture dimensions suggest that a number of CRE sequences are located near or within the rupture patch (Figure 3). It is possible that the true dimensions of the rupture are smaller than the estimate presented here, as the event likely had a relatively high stress drop. The cataloged aftershock sequence is widespread across the fault and does not provide immediate information about the rupture dimensions. However, it is likely that the *M*5.7 rupture zone coincided with at least some of the aseismic zone around the repeaters, meaning that some areas of the fault zone may have deficits to be made up by future seismic slip. The potential quiescence for the 2 years following the *M*5.7 event suggests that this event had relatively little postseismic slip. Interestingly, the possible quiescence following this event extends to CRE sequences many kilometers away from the inferred rupture patch, in regions of the fault interface that should have experienced small Coulomb stress increases after the rupture (Figure 3c). This may be because many sequences happened to have events in late 2014 and early 2015, meaning they were early in their presumed seismic cycle when the *M*5.7 earthquake occurred (Figure 2d). The most recent observations suggest that many CRE sequences resumed activity again in 2017, although it is still too early to completely characterize the interactions between *M*5.7 event and the surrounding CRE sequences.

Our results demonstrate the value of using CREs to monitor for aseismic creep and creep transients where geodetic measurements are not readily available. Although the creep rates we infer are relatively high, they have not been previously documented because land-based geodetic techniques are not well equipped to observe aseismic slip at the offshore MTJ. A back-slip dislocation model (e.g., Okada, 1992) shows that if the MFZ coupling ratio is varied from 0% to 100%, only two currently operating PBO GPS stations would show velocity changes >1 mm/yr (Figure S10). It is thus very difficult to image slip on the MFZ using the existing network of land-based continuous GPS. However, our findings suggest that this region may be well suited for experiments with seafloor geodesy in the future using acoustic ranging or GPS-acoustic systems (Bürgmann & Chadwell, 2014; McGuire & Collins, 2013). The fast deformation rates and high likelihood of aseismic creep make the MFZ a favorable target for these techniques, especially when integrated with constraints from seismicity data and CREs.

5 Conclusion

Repeating microearthquakes provide evidence that the MFZ, an oceanic transform fault, is creeping on average between 2008 and 2017 at about 65% of its long-term slip rate and may display small variations in creep rate over the study period. This evidence of fault creep supports previous suggestions that aseismic moment release is an important mode of slip for oceanic transform systems. Surrounding a nearby M5.7 earthquake on the MFZ, we find that CRE activity may undergo a slight increase and subsequent decrease, but the decrease cannot be explained by static earthquake stress interactions alone. In addition to the MFZ, we detect shallower creep between the Pacific plate and the southern edge of the North American accretionary prism, and several persistent CRE sequences on an intraplate fault in the Gorda subplate. Determining whether the slip rates inferred in this study are transient or representative of longer-term rates will require additional work on older and future datasets. In the complex deformation field of the MTJ, CRE observations can provide an important observational constraint on aseismic slip and its time-dependent variations.

Acknowledgments